Biomedical Materials

Optimization of hybrid gelatin-polysaccharide bioinks exploiting thiol-norbornene chemistry using a reducing additive

To cite this article before publication: Nathan Carpentier *et al* 2024 *Biomed. Mater.* in press https://doi.org/10.1088/1748-605X/ad2211

Optimization of hybrid gelatin-polysaccharide bioinks exploiting thiol-norbornene chemistry using a reducing additive

Nathan Carpentier[1], Laurens Parmentier[1], Louis Van der Meeren[2], André G. Skirtach[2], Peter Dubruel[1], Sandra Van Vlierberghe[1*]

1) Polymer Chemistry & Biomaterials Group, Centre of Macromolecular Chemistry, Department of Organic and Macromolecular Chemistry, Ghent University, 9000 Ghent, Belgium.

2) Nano-Biotechnology Laboratory, Department of Biotechnology, Faculty of Bioscience Engineering, Ghent University, Ghent, Belgium.

[*]Corresponding Author

E-mail: Sandra.VanVlierberghe@UGent.be

Abstract

Thiol-norbornene chemistry offers great potential in the field of hydrogel development, given its step growth crosslinking mechanism. However, limitations exist with regard to deposition-based bioprinting of thiol-containing hydrogels, associated with premature crosslinking of thiolated (bio)polymers resulting from disulfide formation in the presence of oxygen. More specifically, disulfide formation can result in an increase in viscosity thereby impeding the printing process. In the present work, hydrogels constituting norbornene-modified dextran (DexNB) combined with thiolated gelatin (GelSH) are selected as case study to explore the potential of incorporating the reducing agent tris(2-carboxyethyl)phosphine (TCEP), to prevent the formation of disulfides. We observed that, in addition to preventing disulfide formation, TCEP also contributed to premature, spontaneous thiol-norbornene crosslinking without the use of UV light as evidenced via ^{1}H-NMR spectroscopy. Herein, an optimal concentration of 25 mol% TCEP with respect to the amount of thiols was found, thereby limiting auto-gelation by both minimizing disulfide formation and spontaneous thiol-norbornene reaction. This concentration results in a constant viscosity during at least 24 hours, a more homogeneous network being formed as evidenced using atomic force microscopy while retaining bioink biocompatibility as evidenced by a cell viability of human foreskin fibroblasts exceeding 70 % according to ISO 10993-6:2016.

1. Introduction

3D-printing of biomaterials has gained increasing interest in the fields of tissue engineering[1], drug delivery[2] as well as to support the development of in vitro models.[3,4] A major challenge in the field involves the establishment of printable inks starting from materials with suitable rheological properties[5]. In this regard, gelatin exhibits superior processing capabilities due to its upper critical solution temperature (UCST) and shear-thinning behaviour.[6,7] With regard to deposition-based 3D-printing applications, photo-crosslinkable gelatin is often used as it can be printed at temperatures

around 25 °C[8], at which it exhibits a viscosity (≈ 0.15 - 0.10 Pa·s)[9] suitable for printing.[10] Depending on the printing method applied, gelatin can be directly photo-crosslinked[11] (e.g. through stereolithography (SLA)[12] and digital light processing (DLP)[13]) or after a physical gelation step[14] (in case of extrusion-based printing) to maintain its printed shape. Gelatin is also often blended with other materials that exhibit inferior rheological properties[15] with regard to 3D-printing, such as a too low viscosity (<0.03 Pa·s at 25 °C)[16], the absence of shear-thinning behaviour or the lack of physical gelation[17] directly after the material is extruded. Gelatin can also be introduced in a bioink to enhance cell interactivity.[18] To ensure a reproducible extrusion-based printing process, it is desirable that the biomaterial ink formulation exhibits a constant viscosity[19] during printing, situated within a printable range (0.03 Pa·s to 6 × 10^4 Pa·s)[20]. Furthermore, too low viscosity will decrease the printing resolution[21], while too high viscosity will cause nozzle clogging and will obstruct the application of the materials as bioink due to high shear stresses accompanying nozzle-based printing techniques.[22,23]

The most frequently reported photo-crosslinkable gelatin used for bioprinting is methacrylated gelatin (GelMA)[24], although this material holds some disadvantages associated with its chain growth crosslinking mechanism. A superior and currently well-established crosslinking strategy described in literature exploits thiol-norbornene chemistry to develop gelatin-based hydrogels.[25,26,27,28] However, thiol-norbornene crosslinking also poses limitations when exploiting thiol-based crosslinkers prone to disulfide formation in the presence of oxygen (through oxidation) and at elevated temperatures.[29,34]

In the current work, a strategy is established to improve the printability of thiolated gelatin-based hydrogel inks towards printing methods that require constant rheological properties to facilitate reliable and reproducible processing. Tris(2-carboxyethyl)phosphine (TCEP) is exploited as reducing additive[30] to prevent undesired, premature disulfide crosslinking, hence retaining a constant viscosity. As case study, a combination of thiolated gelatin (GelSH) and norbornene-modified dextran (DexNB) was optimized towards deposition-based 3D-printing. The above-mentioned hydrogel was recently reported as starting material for processing into 3D-scaffolds to support liver tissue engineering.[31] Indirect 3D-printed scaffold were printed without any problem, because this technique only required a processing time of around 10 minutes. However, problems were faced regarding the rapid increase in viscosity of the ink formulation when prolonged processing times were applied, thereby leading to an impeded extrusion-based printing process.

2. Material and methods

Materials

Gelatin type B, isolated from bovine skin through an alkaline process was supplied by Rousselot (Ghent, Belgium). Dextran (Mr ~40,000 g/mol) (dextran 40) from Leuconostoc spp., N-acetyl-homocysteine thiolactone, 5-norbornene-2-carboxylic acid, N,N'-dicyclohexylcarbodiimide (DCC), dimethylformamide (DMF), 4-(dimethylamino)pyridine (DMAP), ethylenediaminetetraacetic acid (EDTA), hydroxylamine hydrochloride, Calcein-acetoxymethyl ester (Calcein-AM), propidium iodide (PI) were purchased from Sigma-Aldrich (Diegem, Belgium). Tris(2-carboxyethyl)phosphine (TCEP) was purchased from TCI Europe (Zwijndrecht, België). Spectrapor dialysis membranes with molecular weight cut-off (MWCO) 6 – 8 kDa and 12 – 14 kDa were purchased from Polylab (Antwerp, Belgium). Dulbecco's modified eagle's medium (DMEM) Glutamax, fetal bovine serum (FBS) and antibiotics (penicillin/streptomycin) were purchased from Gibco (California, USA). 3-(4,5-dimethylthiazol-2-yl)-5-(3-carboxymethoxyphenyl)-2-(4-sulfophenyl)-2H-tetrazolium (MTS) assay kit was purchased from Abcam (Cambridge, UK). Human foreskin fibroblasts are purchased from American Type Culture Collection (ATCC).

Development of DexNB

Dextran was modified with norbornene functionalities via conventional N,N'-Dicyclohexylcarbodiimide (DCC)/4-Dimethylaminopyridine (DMAP) coupling chemistry occurring between the hydroxyl groups (of dextran) and the carboxylic acids (of 5-norbornene-2-carboxylic acid).[31] A total of 5 g dextran (0.031 mol anhydroglucose unit (AGU)) was dissolved in 100 mL dry DMF containing 10 w/v% LiCl at 80 °C. After dextran was dissolved and the mixture was cooled to room temperature, 16.7 mmol 5-norbornene-2-carboxylic acid, corresponding to 0.5 eq with respect to the amount of AGU present, was added. Subsequently, 12.3 mmol (0.4 eq) DMAP was added. After the mixture was cooled to 0 °C using an ice bath, 15.4 mmol (0.5 eq) of N,N'-dicyclohexylcarbodiimide (DCC) was added. After 48 h reaction, impurities were precipitated in 500 mL double-distilled water and filtered out. The filtrate was dialyzed using a molecular weight cutoff (MWCO) membrane of 6−8 kDa over a period of 1 week against distilled water. The product was isolated by freeze-drying. DexNB with a degree of substitution (DS) of 16% in according the amount of anhydroglucose units was obtained.

Development of GelSH

GelSH was developed according to a protocol described earlier by Van Vlierberghe et al.[32] Briefly, 10 g gelatin type B was dissolved at 40 °C in 100 mL 0.02 M carbonate buffer (pH 10). A total of 15 mM of EDTA was added to the reaction mixture. Subsequently, 5 eq of N-acetyl-homocysteine thiolactone were added to the reaction mixture followed by stirring during 3 h. After 3 h, 100 mL of double-distilled water was added and dialysis against distilled water was performed during 24 h at 40 °C under an inert argon atmosphere using a MWCO membrane of 12−14 kDa. After dialysis, the purified mixture was frozen using liquid nitrogen and freeze-dried. GelSH with a degree of substitution (DS) of 65 % in according to the amount of amines present in gelatin was obtained.

^{1}H-NMR spectroscopy

The degree of substitution (DS) of DexNB was determined using a 400 MHz Bruker Avance II Ultrashield ^{1}H-NMR spectrometer at room temperature via the following formula:

$$DS\ DexNB\ (\%) = \frac{\left(\frac{I_{6.0\ ppm} + I_{6.3\ ppm}}{2}\right)}{I_{4.9\ ppm}}\ x\ 100$$

OPA analysis

The ortho-phthalic dialdehyde (OPA) assay is a spectrophotometric assay to quantify the amount of amines present in a sample enabling to calculate the DS of the different gelatin derivatives. 20 mg OPA was dissolved in 10 mL ethanol and diluted to a final volume of 50 mL with double distilled water. In a second stock solution, 25 µL of 2-mercaptoethanol was added to 50 mL borate buffer (0.1 M, pH 10). The reference in this assay contained 1000 µL double distilled water, 1500 µL 2-mercaptoethanol solution and 500 µL OPA solution. A calibration curve was obtained by comparing the reference samples to a sample containing 50 µL n-butylamine standard solutions (0.002 M, 0.006 M, 0.01 M), 950 µL double distilled water, 1500 µL 2-mercaptoethanol solution and 500 µL OPA solution. The absorbance of the samples at 335 nm was measured using a spectrophotometer and a calibration curve was plotted. Solutions were made of gelatin type B, GelMA and GelSH at a concentration of 25 mg/mL. Samples were measured with the spectrophotometer containing 50 µL of the gelatin solutions, 950 µL double distilled water, 1500 µL 2-mercaptoethanol solution and 500 µL OPA solution at 335 nm. All measurements were performed in triplicate and at 37 °C.

Preparation of hydrogel precursor solution

All hydrogels used throughout this work (i.e. DexNB-GelSH and DexNB-DTT) were UV-A crosslinkable in the presence of a photoinitiator (PI). The hydrogels were prepared starting from an aqueous solution with a total polymer concentration of 10 w/v %. 2 mol % of Lithium phenyl-2,4,6-trimethylbenzoylphosphinate (LAP) as PI was added to the precursor solution, unless stated otherwise. All hydrogel precursor solutions were prepared with equimolar reactive moieties, meaning that the molar amounts of thiols and norbornene functionalities were identical (i.e. #eq. NB = #eq. SH).

Atomic Force Microscopy

Atomic Force Microscopy (AFM) measurements were performed using the Nanowizard 4 instrument (JPK-bioAFM, Bruker), in order to analyze nanoscale morphological and mechanical properties. For all measurements the DNP-10 (Bruker) chip is used from which triangular cantilever A (hard samples: nominal spring constant 0.35 N/m) and cantilever c (soft samples: nominal spring constant 0.24 N/m). The AFM measurements were performed in the Quantitative Imaging mode (QI-mode). This mode allows to simultaneously gather information on morphological and mechanical properties. All data processing was performed in the JPK SPM DP software (image processing, roughness calculation, Young's modulus calculation). To calculate the elasticity (the Young's modulus [kPa]) of the samples, the Hertz/Sneddon model for parabolical indenters is used.

Determination of gel fraction

2D-discs were freeze-dried after crosslinking and weighed. The obtained mass is the mass before leaching out of the non-crosslinked compounds (w_1). Swelling these samples during 24 hours at 37 °C in double distilled water and weighing them after another freeze-drying step resulted in the mass of the samples after leaching out of the non-crosslinked compounds (w_2).

The gel fraction can be calculated by the following formula (n = 6):

$$Gel\ fraction = \frac{w_2}{w_1} . 100$$

Determination of swelling ratio

The swelling ratio was determined using the following protocol. The samples were weighed after freeze-drying (w_d) and after swelling for 24 hours at 37 °C in PBS (w_s). The gel fraction can be calculated using the following formula (n = 6):

$$mass\ swelling\ ratio = \frac{(w_s - w_d)}{w_d}$$

Rheology experiments

In-situ UV-crosslinking

A rheometer-type Physica MCR-301 was applied. For in situ photorheology, 300 µL of each solution was placed between the plates of the device using a gap setting of 0.3 mm. An oscillation frequency of 1 Hz and a strain of 0.1% were applied. The samples were irradiated at 37 °C using a UV-A light (10 min, 3500 mW/cm^2, 365 nm), followed by 2 min of postcuring monitoring. All measurements were performed in triplicate.

Viscosity measurement

The viscosity of the formulations was determined using a rheometer type Physica MCR 310 (Anton Paar, Belgium). The gap width between the lower fixed plate and the rotating spindle (⌀ 15 mm) was

set to 0.3 mm. The shear rate of the spindle was increased from 1 to 1000 s^{-1}. The temperature during the measurements was 25 °C, which was representative for the printing temperature exploited during bioprinting.[33] All measurements were performed in triplicate.

Cell culture protocols

Culturing of cells

Dulbecco's modified Eagle medium supplemented with 10% (v/v) fetal bovine and 1% (v/v) penicillin/streptomycin was used to culture human foreskin fibroblasts at 37 °C in 5% CO_2. Every 3 days, the culture medium was changed until 80–90% confluency was reached, which was followed by subculturing.

MTS proliferation assay

The 3-(4,5-Dimethylthiazol-2-yl)-5-(3-carboxymethoxyphenyl)-2-(4-sulfophenyl)-2H-tetrazolium (MTS) assay kit was thawed. The medium was aspirated from the wells, and 250 µL of fresh medium was added, after which 40 µL of the MTS solution was added to the fresh medium of the wells. After an incubation time of 3 h at 37 °C, 100 µL of the medium/MTS mixture of each well was transferred to the wells of a 96-well plate. The absorbance was measured in triplicate at 490 nm using a spectrophotometer.

Live/dead staining

The cytocompatibility of the hydrogels was tested through a live/dead assay using calcein acetoxymethyl ester (calcein-AM) and propidium iodide (PI) staining. For every 1 mL of PBS, 2 µL of calcein-AM and 2 µL of PI were added. A 48-well plate was used and 0.3 mL of the solution was added to each well. The wells were incubated in the dark at room temperature for 10 min. A fluorescence microscope with a green fluorescence protein (GFP) filter for calcein was used to visualize the living cells. A Texas Red (TxRed) filter was used to visualize the dead cells using PI. Image processing was performed using ImageJ software.

3D-printing

A printing test was performed evidencing the superior printability of the optimized hydrogel precursor solution using a BioX bioprinter from Cellink. The printing parameters were optimized for the hydrogel precursor solution directly after preparing the solution. The same parameters for printing the constructs were applied for all hydrogel precursor solutions 10 hours after preparing the solutions. The following parameters were applied for all the printed constructs:

Printer	BioX Cellink
Printing temperature	25 °C
Printing speed	10 mm/s
Pressure	150 Pa
Build plate temperature	8 °C
Nozzle diameter	21 Gauge

Statistical analysis

All measurements were performed in triplicate and the average values are plotted. Significant differences were determined using a student's t-test. $P < 0.05$ indicates a significant difference.

3. Results and discussion

When exploiting thiol-based bioink formulations to develop thiol-norbornene hydrogels, an increase in viscosity hampers its processing capability. Since it is hypothesized that this phenomenon is due to

thiol oxidation leading to undesired, premature disulfide crosslinking in the presence of oxygen[34], the effect of adding TCEP as a reducing agent on the viscosity of thiolated gelatin solutions was investigated. 0, 0.05 and 0.5 equivalents of TCEP were added to a 10 w/v% GelSH solution with a degree of substitution (DS) of 60 % as confirmed by OPA analysis (see Figure 1). As anticipated, the viscosity of a GelSH solution without TCEP increased significantly from 0.43 ± 0.04 Pa·s at the first time point up to 12 ± 3 Pa·s after 24 hours. When 0.5 eq of TCEP was added, the viscosity remained constant ($p > 0.05$) with a value of 0.15 ± 0.03 Pa·s at the first time-point and 0.12 ± 0.03 Pa·s after 24 hours. When 0.05 eq was added, the increase in viscosity was less pronounced, albeit significant from 0.36 ± 0.02 Pa·s up to 0.85 ± 0.06 Pa·s within the same time frame.

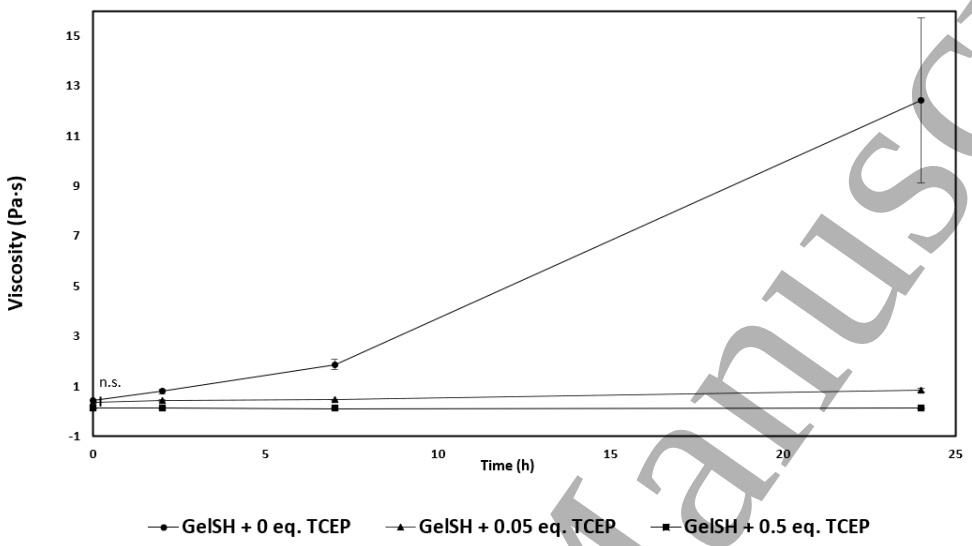

Figure 1: Viscosity of a 10 w/v% GelSH solution as a function of time in the absence and presence of 0.05 and 0.5 eq. TCEP. In the absence of TCEP, a rapidly increasing viscosity is observed over time, while 0.05 eq. resulted in a viscosity increase, albeit to a lesser extent, and 0.5 eq. resulted in a constant viscosity for at least 24 hours. (N=3)

Subsequently, the effect of the addition of TCEP on a hydrogel precursor solution exploiting thiol-norbornene crosslinking was studied using GelSH and DexNB as crosslinkable building blocks. DexNB exhibited a DS of 15 % as confirmed by ^{1}H-NMR spectroscopy. As anticipated, the viscosity of the DexNB-GelSH precursor solution increased from 0.17 ± 0.04 Pa·s up to 0.86 ± 0.12 Pa·s over 6 hours in the absence of TCEP due to the formation of disulfides. Surprisingly, when adding 0.5 equivalents of TCEP, the viscosity of the solution increased as well. Over 6 hours, the viscosity increased from 0.140 ± 0.002 Pa·s up to 1.12 ± 0.27 Pa·s. This phenomenon might be explained by a spontaneous thiol-norbornene reaction taking place in the absence of a photo-initiator nor upon applying UV-A irradiation. In 2017, this phenomenon of spontaneous thiol-norbornene reaction was described for the first time by McOscar et al.[35] reporting on the reaction of carbic carboxymethylcellulose with 2,2'-(ethylenedioxy)diethanethiol. The authors suggested the thiol-olefin co-oxidation (TOCO)[36] with oxygen from air as underlying mechanism, although the exact mechanism remains yet to be determined.

The addition of different equivalents of TCEP was evaluated in order to identify the optimal concentration minimizing premature spontaneous crosslinking originating from both disulfide formation and the spontaneous thiol-norbornene reaction, thereby leading to a constant viscosity over time as shown in Figure 2. All DexNB-GelSH solutions exhibited initially a similar viscosity (i.e. not significantly different). At the second time point (3 hours), the formulation not containing TCEP exhibited the highest increase in viscosity (from 0.17 ± 0.04 Pa·s to 0.38 ± 0.08 Pa·s) which was significantly higher compared to that of the other formulations. Moreover, the viscosity of the

formulation containing 0.05 eq. TCEP was significantly higher (from 0.144 ± 0.003 Pa·s to 0.181 ± 0.006) Pa·s) compared to that of formulations containing 0.5 and 0.25 eq TCEP. We hypothesize that in case of the formulations containing 0.05 eq, the TCEP was already consumed after the first time point and thiols started to form disulfide bonds. It is known that TCEP is an irreversible reducing agent, and will retain its oxidized form.[37] At the third time point (6 hours), the viscosity of the formulation containing 0.5 eq. TCEP increased from 0.140 ± 0.002 Pa·s to 1.12 ± 0.27 Pa·s. We hypothesize that this is caused by the presence of a significant amount of free thiols, which stimulated the spontaneous thiol-NB reaction (*vide supra*) leading to an increased viscosity. The formulation containing 0.05 eq. of TCEP increased significantly in viscosity at time points 3 and 4 through further oxidation of the thiols, from 0.230 ± 0.005 Pa·s to 0.365 ± 0.026 Pa·s, while the formulation not containing TCEP increased much faster in viscosity (from 0.862 ± 0.122 Pa·s to 1.94 ± 0.23 Pa·s). Also the viscosity of the formulation containing 0.5 eq. increased further (from 1.12 ± 0.27 Pa·s to 1.43 ± 0.01 Pa·s), while adding 0.25 eq. ensured a constant viscosity for DexNB-GelSH during at least 24 hours (i.e. 0.143 ± 0.02 Pa·s versus 0.154 ± 0.001 Pa·s respectively). The incorporation of lower or higher TCEP amounts led to an increased viscosity over time.

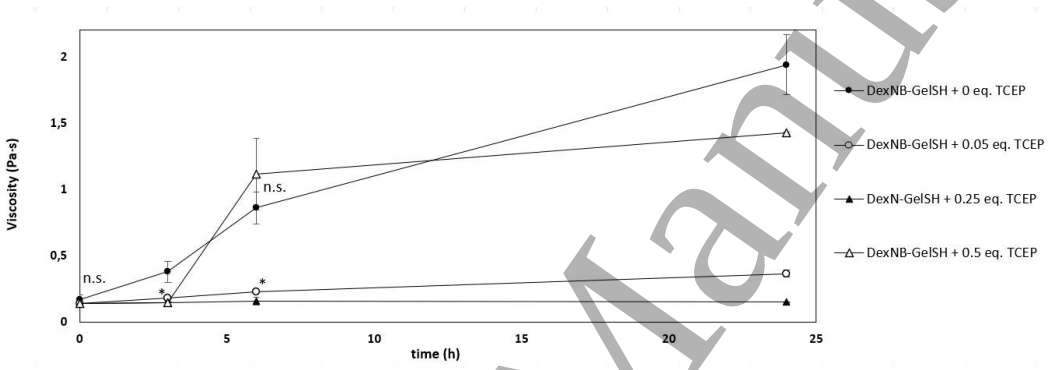

Figure 2: Viscosity at 25°C determined through rheology as a function of time of DexNB-GelSH in the presence of 0, 0.05, 0.25 and 0.5 eq. TCEP ($p < 0.05$). For the optimal concentration of 0.25 eq. TCEP, a constant viscosity is observed for at least 24 hours. Higher or lower TCEP concentrations gave rise to a significant increase in viscosity over time. (N= 3)

Since we hypothesized that the increase in viscosity for the hydrogel precursor solution containing 0.5 eq. TCEP is caused by a spontaneous reaction occurring between thiol and norbornene moieties, this was confirmed by monitoring the reaction between DexNB and dithiothreitol (DTT) during 6 days while being protected from light, in the absence of a PI. This specific composition (i.e. DTT and DexNB) was exploited as proof-of-concept for a thiol-NB reaction, since it enabled the straightforward interpretation of ^{1}H-NMR spectra showing characteristic peaks (NB peaks at 5.9 and 6.2 ppm, DTT peaks around 2.6 and 2.9 ppm and the reference peak corresponding to the anomeric hydrogen atom of dextran[38] at 4.9 ppm), in contrast with the complex ^{1}H-NMR spectrum resulting from DexNB-GelSH due to overlap of gelatin peaks with the reference peak of dextran.[31] As shown in Figure 3, the integration of the hydrogens associated with norbornene decreased over time. All spectra were normalized to the reference peak at 4.9 ppm, corresponding with an integration of 1. It could be calculated from these spectra that the amount of norbornene groups was reduced from 0.93 mol/g to

0.15 mol/g after 6 days which corresponds to 0.78 mol/g norbornene groups that have reacted spontaneously with the thiols of DTT in the absence of a photo-initiator or UV-A irradiation.

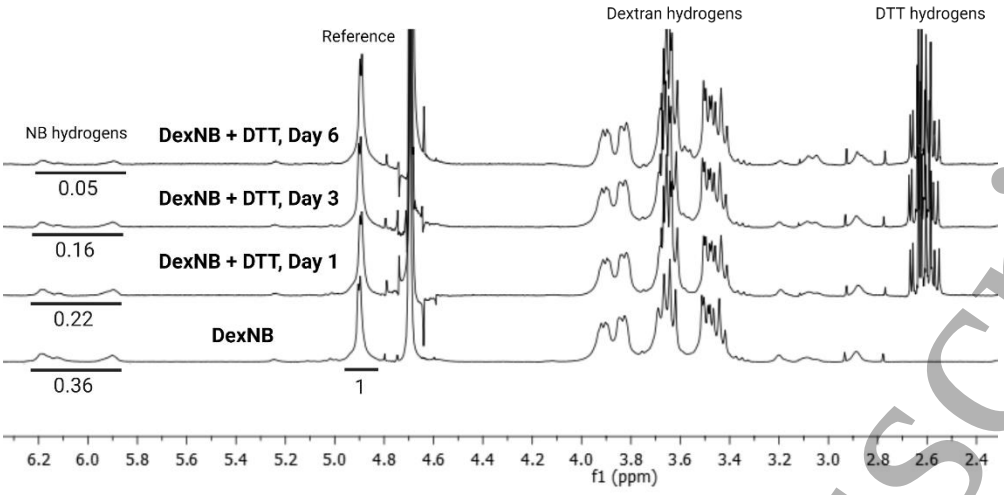

Figure 3: Reaction progress between DexNB and DTT. The reference peak of the anomeric hydrogen atom of dextran (4.9 ppm) integrates for 1 proton in every spectrum. The integrations of the NB peaks around 5.9 and 6.2 ppm decrease over time pointing towards spontaneous thiol-NB reaction.

To investigate the potential influence of TCEP on the UV-A crosslinking reaction of the DexNB-GelSH hydrogel precursor solution (10 w/v% in the presence of a PI), an in situ photo-rheology experiment was performed in the presence and absence of TCEP (see figure 4 left panel, only one of each triplicate is shown). Based on the experiment, the storage modulus after crosslinking was determined. DexNB-GelSH + 0 eq TCEP (i.e. 10.06 ± 0.88 kPa) and DexNB-GelSH + 0.25 eq TCEP (i.e. 9.15 ± 0.23 kPa) did not exhibit a significant difference ($p > 0.05$) in storage modulus. Furthermore, a gel fraction test revealed that the crosslinking efficiency was similar (non-significant) for both hydrogel formulations (see figure 4 right panel). It could be concluded that adding the optimal amount of 0.25 eq of TCEP ensured a constant viscosity over at least 24 hours without compromising the physico-chemical properties of the final hydrogel.

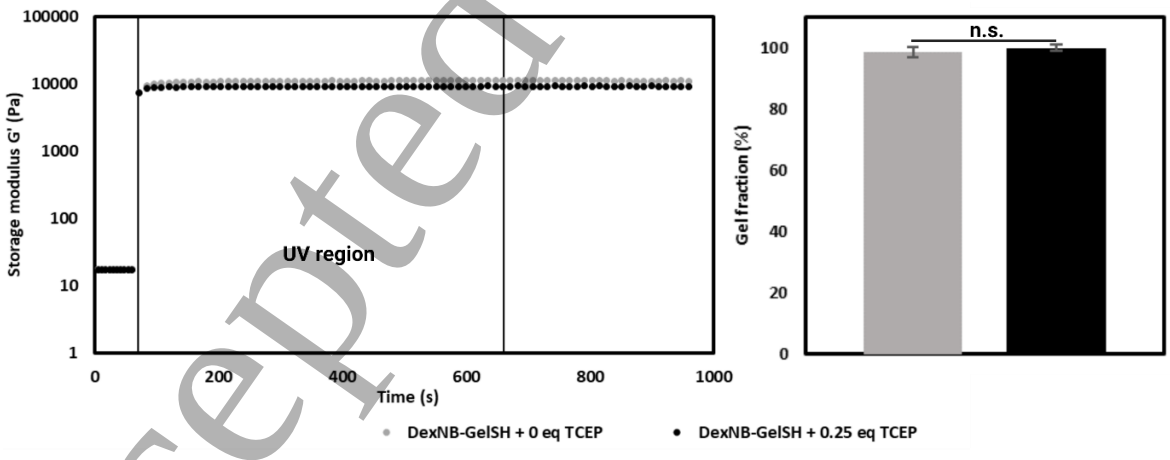

Figure 4: In situ photo-rheology of DexNB-GelSH without TCEP and with 0.25 eq. of TCEP. There is no significant effect on the storage modulus after crosslinking when adding the optimized concentration of TCEP. (left panel). Gel fraction of the two hydrogel formulations. No significant effect on the gel fractions was observed when the optimized concentration of TCEP was added (right panel).

It can be anticipated that, when the optimized amount of TCEP is added to the DexNB-GelSH hydrogel precursor solution, thiol-NB bonds are formed solely during crosslinking instead of additional crosslinks

occurring between GelSH and GelSH. The latter is prevented by the reducing capacity of TCEP. Consequently, this is expected to result in a more homogeneous network. Indeed, due to the orthogonal nature of the thiol-norbornene reaction, dextran and gelatin were forced to exclusively react with one another. The homogeneous network formation is also visualized by AFM showing the elastic moduli along the surface of hydrogel films (see Figure 5). The elastic modulus of DexNB-GelSH in the absence and presence of 0.25 eq of TCEP was respectively 48.1 ± 14.8 kPa and 28.4 ± 7.0 kPa as calculated by the root mean square (RMS) derived from the AFM-recorded stiffness data. These values were not significantly different ($p > 0.05$).

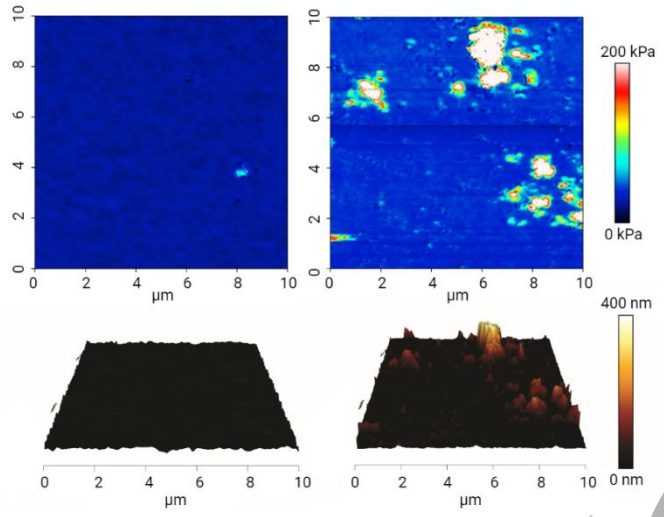

Figure 5: AFM-recorded stiffness (upper panel), and AFM-recorded roughness (lower panel) of a DexNB-GelSH hydrogel containing 0.25 eq TCEP (left) versus in the absence of TCEP (right). The surface plot of the topography showed a more homogeneous surface when the optimized concentration of TCEP was added, whereas TCEP did not have a significant effect on the AFM-recorded young's modulus of the resulting hydrogel according to the stiffness plot along the surface.

To serve as a proof-of-concept, a two-layered scaffold was printed which confirmed the importance of ensuring a constant viscosity on the printing performance.[39,40] The different formulations (with photo-initiator) were printed after 10 hours exploiting the same printing parameters as optimized for the precursor solutions directly after preparation. As shown in Figure 6, the hydrogel formulation containing 0.25 eq. of TCEP resulted in a more homogenous extrusion, a better defined computer-aided design/computer-aided manufacturing (CAD/CAM) mimicry and better defined pores and struts.

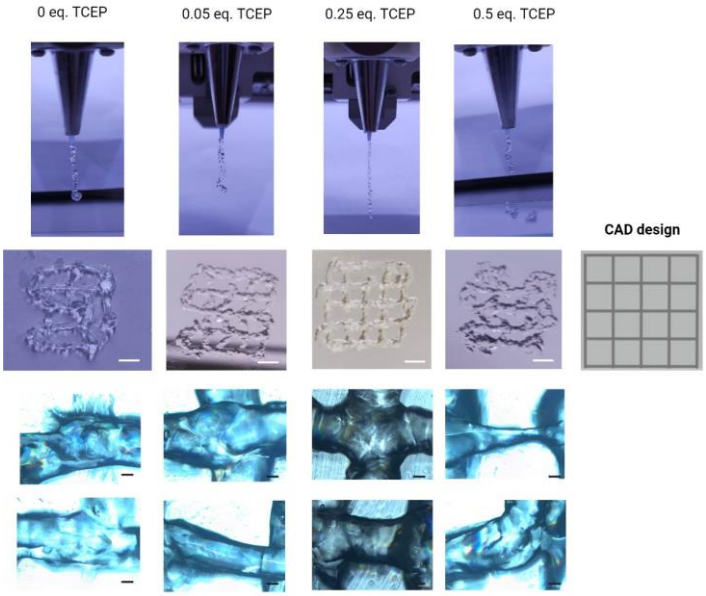

Figure 6: Images of extrusion from the nozzle, the resulting printed constructs and optical microscopy images of the printed constructs exploiting the different biomaterial ink formulations. These images revealed a superior CAD/CAM mimicry for the hydrogel scaffold printed from a formulation constituting 0.25 eq. of TCEP due to the constant viscosity of the ink over time. The white scale bars represent 2.5 mm, the black scale bars represent 500 µm.

Finally, it is of utmost importance that the resulting hydrogel formulations are biocompatible to ensure their applicability in the field of bioprinting.[41] It is known from previous research that DexNB-GelSH is biocompatible.[31] Herein, the cytotoxicity of TCEP is investigated in direct contact with cells. Therefore, the biocompatibility was assessed for different TCEP concentrations (i.e. 0.25, 0.5, 1, 2, 5 and 10 mg/mL corresponding to respectively 0.05, 0.1, 0.2, 0.4, 1 and 2 eq. according to the amount of thiols) present in culture medium for 24 hours exploiting human foreskin fibroblasts (see Figure 7). Up to a concentration of 2 mg/mL TCEP, only a small drop in cell viability was observed, while retaining biocompatibility according to ISO 10993-6:2016 (i.e. viability > 70% in comparison to the control, tissue culture plastic (TCP))[42]. The determined optimal amount of 0.25 equivalents to be added (*vide supra*) corresponds to a concentration of 1.3 mg/mL required for the DexNB-GelSH hydrogel formulation. The latter is situated within the biocompatibility range of TCEP rendering it a suitable hydrogel composition for bioprinting. In addition to the physico-chemical properties of the hydrogel, the biocompatibility is thus also preserved upon incorporating TCEP.

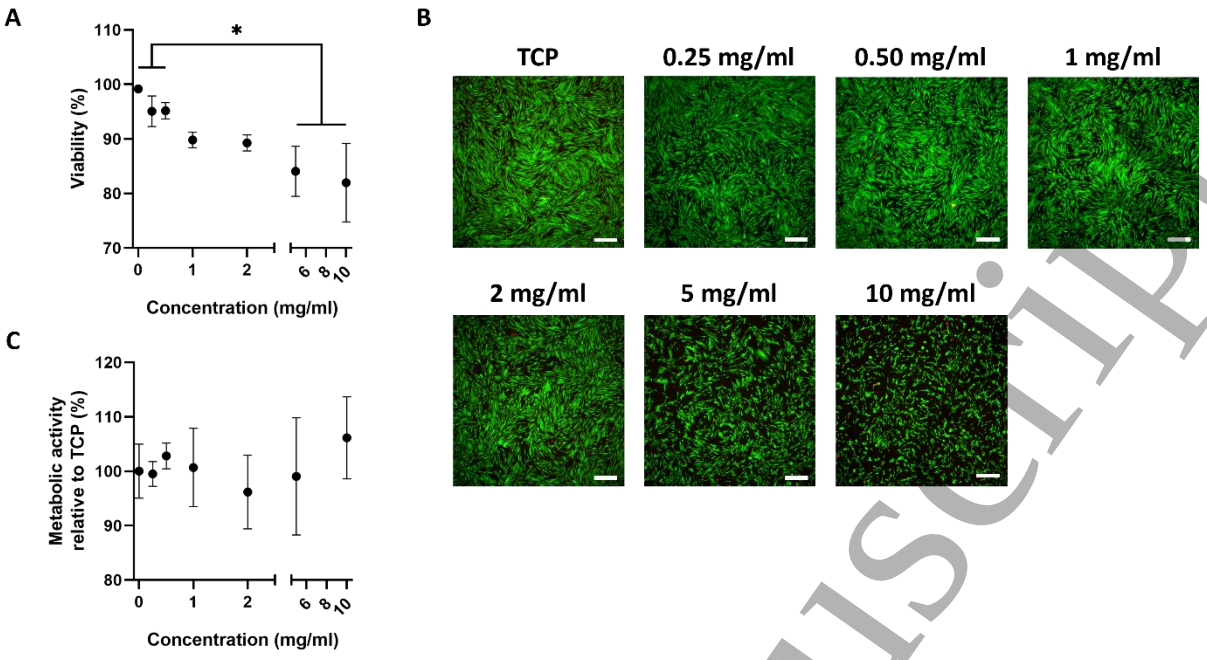

Figure 7: Effect of different TCEP concentrations on human foreskin fibroblasts assessed via a Live/Dead assay (A and B) and a MTS proliferation assay (C). The results revealed that the optimized TCEP concentration does not compromise cell viability according to ISO 10993-6:2016. ($p<0.05$). (N=3) (Scale bars represent 500 µm)

4. Conclusions and future perspectives

In the present work, we investigated the autogelation occurring in thiol-norbornene hydrogel precursor solutions exploiting a DexNB-GelSH hydrogel as case study. We confirmed that this process encompasses a combination of both disulfide formation in the presence of oxygen as well as the spontaneous reaction occurring between thiol and norbornene moieties. We herein suggested a solution to prevent the oxidation of thiolated biopolymers while minimizing the spontaneous thiol-norbornene reaction through only a minor modification of existing formulations. Through the incorporation of 0.25 eq TCEP to the hydrogel precursor solution, premature crosslinking could be avoided and a long-term constant viscosity over at least 24 hours was ensured. Furthermore, this optimized composition resulted in superior printing performance as evidenced by a printing test using a pressure assisted deposition-based 3D-printing technique. Furthermore, the optimized hydrogel formulation retained its biocompatibility towards human fibroblasts. Interestingly, this strategy could potentially also be applied beyond the herein exploited GelSH and DexNB biopolymers offering a straightforward solution for all hydrogel inks encompassing thiolated polymers.

5. Data availability statement

All data that support the findings of this study are included within the article, or can be achieved from the corresponding author upon request.

6. Acknowledgements

NC and LP would like to acknowledge the Research Foundation Flanders (FWO) for providing an FWO-SB fellowship (3S99321N and 1S44221N). AGS acknowledges support of FWO (I002620N).

7. References

1 N. Poomathi, S. Singh, C. Prakash, A. Subramanian, R. Sahay, A. Cinappan and S. Ramakrishna,

3D printing in tissue engineering : a state of the art review of technologies and biomaterials, *Rapid Prototyp. J. Rep.*, , DOI:10.1108/RPJ-08-2018-0217.

2 A. Etxabide, J. Long, P. Guerrero, K. De and A. Seyfoddin, 3D printed lactose-crosslinked gelatin sca ff olds as a drug delivery system for dexamethasone, *Eur. Polym. J.*, 2019, **114**, 90–97.

3 Y. Choi, H. Park, D. Ha, H. Yun and H. Yi, 3D Bioprinting of In Vitro Models Using Hydrogel-Based, *Polymers (Basel).*, , DOI:10.3390/polym13030366.

4 N. Carpentier, L. Urbani, P. Dubruel and S. Van Vlierberghe, Biomaterials Science The native liver as inspiration to create superior in vitro hepatic models, *Biomater. Sci.*, 2023, **11**, 1091–1115.

5 K. Hölzl, S. Lin, L. Tytgat, S. Van Vlierberghe, L. Gu and A. Ovsianikov, Bioink properties before , during and after 3D bioprinting, *Biofabrication*, , DOI:10.1088/1758-5090/8/3/032002.

6 Y. Zhang, H. Chen and J. Li, Recent advances on gelatin methacrylate hydrogels with controlled microstructures for tissue engineering, *Int. J. Biol. Macromol.*, 2022, **221**, 91–107.

7 S. Chatterjee and P. C. Hui, Review of Applications and Future Prospects of Stimuli-Responsive Hydrogel Based on Thermo-Responsive Biopolymers in Drug Delivery Systems, *Polymers (Basel).*, 2021, **13**, 13132086.

8 L. Tytgat, L. Van Damme, J. Van Hoorick, H. Declercq, H. Thienpont, H. Ottevaere, P. Blondeel, P. Dubruel and S. Van Vlierberghe, Additive manufacturing of photo-crosslinked gelatin scaffolds for adipose tissue engineering, *Acta Biomater.*, 2019, **94**, 340–350.

9 C. Barrera, V. Florián-Algarin, A. Acevedo and C. Rinaldi, Monitoring gelation using magnetic nanoparticles, *Soft Matter*, 2010, **6**, 3662–3668.

10 N. Rajabi, A. Rezaei, M. Kharaziha, H. R. Bakhsheshi-rad, H. Luo, S. Ramakrishna and F. Berto, Recent Advances on Bioprinted Gelatin Methacrylate-Based Hydrogels for Tissue Repair, *Tissue Eng. - Part A*, 2021, **27**, 679–702.

11 H. Kumar, K. Sakthivel, M. G. A. Mohamed, E. Boras, S. R. Shin and K. Kim, Designing Gelatin Methacryloyl (GelMA) -Based Bioinks for Visible Light Stereolithographic 3D Biofabrication, *Macromol. Biosci.*, 2020, **21**, 1–17.

12 H. Kumar, K. Sakthivel, M. G. A. Mohamed, E. Boras, S. R. Shin and K. Kim, Designing Gelatin Methacryloyl (GelMA) -Based Bioinks for Visible Light Stereolithographic 3D Biofabrication, 2021, **2000317**, 1–17.

13 P. Song, M. Li, B. Zhang, X. Gui, Y. Han, L. Wang, W. Zhou, L. Guo, Z. Zhang, Z. Li and C. Zhou, DLP fabricating of precision GelMA / HAp porous composite scaffold for bone tissue engineering application, *Compos. Part B*, 2022, **244**, 110163.

14 A. T. Young, O. C. White and M. A. Daniele, Rheological Properties of Coordinated Physical Gelation and Chemical Crosslinking in Gelatin Methacryloyl (GelMA) Hydrogels, *Macromol. Biosci.*, 2020, **20**, 1–15.

15 D. Chimene, K. K. Lennox, R. R. Kaunas and A. K. Gaharwar, Advanced Bioinks for 3D Printing : A Materials Science Perspective, *Ann. Biomed. Eng.*, 2016, **44**, 2090–2102.

16 J. Yin, M. Yan, Y. Wang, J. Fu and H. Suo, 3D Bioprinting of Low-Concentration Cell-Laden Gelatin Methacrylate (GelMA) Bioinks with a Two-Step Cross-linking Strategy, *ACS Appl. Mater. Interfaces*, 2018, **10**, 6849–6857.

17 W. Liu, M. A. Heinrich, Y. Zhou, A. Akpek, N. Hu and X. Liu, Extrusion Bioprinting of Shear-

Thinning Gelatin Methacryloyl Bioinks, *Adv. Healthc. Mater.*, 2017, **6**, 1601451.

18 A. B. Bello, D. Kim, D. Kim, H. Park and S. Lee, Engineering and Functionalization of Gelatin Biomaterials : From Cell Culture to Medical Applications, 2020, **26**, 164–180.

19 D. Hardman, J. Hughes, T. G. Thuruthel and K. Gilday, 3D Printable Sensorized Soft Gelatin Hydrogel for Multi-Material Soft Structures, *Robot. Autom. Lett.*, 2021, **6**, 5269–5275.

20 S. V. Murphy and A. Atala, 3D bioprinting of tissues and organs, *Nat. Biotechnol.*, 2014, **32**, 773–785.

21 B. Stolz, F. Mönkemeyer, M. Mader, S. Schmidt, L. Volk, T. Steinberg, B. Bruchmann and R. Mülhaupt, Polyhydroxymethylenes as Multifunctional High Molecular Weight Sugar Alcohols Tailored for 3D Printing and Medical Applications, *Macromol. Chem. Phys.*, 2020, 2000132.

22 I. Gorroñogoitia, U. Urtaza, A. Zubiarrain-laserna, A. Alonso-varona and A. M. Zaldua, A Study of the Printability of Alginate-Based Bioinks by 3D Bioprinting for Articular Cartilage Tissue Engineering, 2022, 1–17.

23 B. Duan, E. Kapetanovic, L. A. Hockaday and J. T. Butcher, Three-dimensional printed trileaflet valve conduits using biological hydrogels and human valve interstitial cells, *Acta Biomater.*, 2014, **10**, 1836–1846.

24 A. I. Van Den Bulcke, B. Bogdanov, N. De Rooze, E. H. Schacht, M. Cornelissen and H. Berghmans, Structural and rheological properties of methacrylamide modified gelatin hydrogels, *Biomacromolecules*, 2000, **1**, 31–38.

25 L. Van Damme, J. Van Hoorick, P. Blondeel and S. Van Vlierberghe, Toward Adipose Tissue Engineering Using Thiol-Norbornene Photo- Crosslinkable Gelatin Hydrogels, *Biomacromolecules*, 2021, **22**, 2408–2418.

26 T. Greene and C. C. Lin, Modular Cross-Linking of Gelatin-Based Thiol-Norbornene Hydrogels for in Vitro 3D Culture of Hepatocellular Carcinoma Cells, *ACS Biomater. Sci. Eng.*, 2015, **1**, 1314–1323.

27 J. Van Hoorick, P. Gruber, M. Markovic, M. Rollot, G. J. Graulus, M. Vagenende, M. Tromayer, J. Van Erps, H. Thienpont, J. C. Martins, S. Baudis, A. Ovsianikov, P. Dubruel and S. Van Vlierberghe, Highly Reactive Thiol-Norbornene Photo-Click Hydrogels: Toward Improved Processability, *Macromol. Rapid Commun.*, 2018, **39**, 1800181.

28 J. Van Hoorick, A. Dobos, M. Markovic, T. Gheysens and L. Van Damme, Thiol-norbornene gelatin hydrogels : influence of thiolated crosslinker on network properties and high definition 3D printing Thiol-norbornene gelatin hydrogels : influence of thiolated crosslinker on network properties and high definition 3D printing, *Biofabrication*, 2021, **13**, 1–22.

29 T. Göckler, S. Haase, X. Kempter, R. Pfister, B. R. Maciel, A. Grimm, T. Molitor, N. Willenbacher and U. Schepers, Tuning Superfast Curing Thiol-Norbornene-Functionalized Gelatin Hydrogels for 3D Bioprinting, 2021, **2100206**, 1–13.

30 F. Goethals, D. Frank and F. Du Prez, Progress in Polymer Science Protected thiol strategies in macromolecular design, *Prog. Polym. Sci.*, 2017, **64**, 76–113.

31 N. Carpentier, L. Van Der Meeren, A. G. Skirtach, L. Devisscher, H. Van Vlierberghe, P. Dubruel and S. Van Vlierberghe, Gelatin-Based Hybrid Hydrogel Scaffolds: Toward Physicochemical Liver Mimicry, *Biomacromolecules*, , DOI:10.1021/acs.biomac.2c00643.

32 S. Van Vlierberghe, E. Schacht and P. Dubruel, Reversible gelatin-based hydrogels : Finetuning of material properties, *Eur. Polym. J.*, 2011, **47**, 1039–1047.

33 L. Van Damme, E. Briant, P. Blondeel and S. Van Vlierberghe, Indirect versus direct 3D printing of hydrogel scaffolds for adipose tissue regeneration, *MRS Adv.*, 2020, **5**, 855–864.

34 K. Pulka-Ziach, Influence of reaction conditions on the oxidation of thiol groups in model peptidomimetic oligoureas, *J. Pept. Sci.*, 2018, **24**, 4–7.

35 T. Mcoscar, The University of Maine, 2017.

36 V. T. D'Souza, R. Nanjundiah, J. Baeza and H. H. Szmant, Thiol-Olefin Cooxidation (TOCO) Reaction. 9. A Self-consistent Mechanism under Nonradical-Inducing Conditions, *J. Org. Chem.*, 1987, **52**, 1729–1740.

37 D. J. Cline, S. E. Redding, S. G. Brohawn, J. N. Psathas, J. P. Schneider and C. Thorpe, New water-soluble phosphines as reductants of peptide and protein disulfide bonds: Reactivity and membrane permeability, *Biochemistry*, 2004, **43**, 15195–15203.

38 H. L. Ramirez, A. Valdivia, R. Cao and A. Fragoso, Preparation of β -Cyclodextrin-Dextran Polymers and their Use as Supramolecular Carrier Systems for Naproxen Preparation of β -Cyclodextrin-Dextran Polymers and their Use as Supramolecular Carrier Systems for Naproxen, *Polym. Bull.*, 2007, **59**, 597–605.

39 S. Kyle, Z. M. Jessop, A. Al-sabah and I. S. Whitaker, 'Printability' of Candidate Biomaterials for Extrusion Based 3D Printing: State-of-the-Art, *Adv. Healthc. Mater.*, 2017, **6**, 1700264.

40 L. Ouyang, R. Yao, Y. Zhao and W. Sun, Effect of bioink properties on printability and cell viability for 3D bioplotting of embryonic stem cells Effect of bioink properties on printability and cell viability for 3D bioplotting of embryonic stem cells, *Biofabrication*, 2016, **8**, 035020.

41 A. S. Theus, L. Ning, B. Hwang, C. Gil, S. Chen, A. Wombwell, R. Mehta and V. Serpooshan, Bioprintability : Physiomechanical and Biological Requirements of Materials for 3D Bioprinting Processes, *Polymers (Basel).*, 2020, **12**, 2262.

42 P. Moerbeck-filho, S. C. Sartoretto and M. J. Uzeda, Evaluation of the In Vivo Biocompatibility of Amorphous Calcium Phosphate-Containing Metals, *J. Funct. Biomater.*, 2020, **11**, 11020045.